Published in final edited form as:
Anal Chem. 2010 June 15; 82(12): 5012–5019. doi:10.1021/ac1010316.

Direct DNA Methylation Profiling Using Methyl Binding Domain Proteins

Yinni Yu[†], **Steve Blair**[*,†,‡], **David Gillespie**[¶], **Randy Jensen**[¶], **David G. Myszka**[§], **Ahmed H. Badran**[‖], **Indraneel Ghosh**[‖], and **Alexander Chagovetz**[⊥]

[†]Department of Bioengineering, University of Utah, 72 South Central Campus Drive, Room 2750, Salt Lake City, UT 84112

[‡]Department of Electrical and Computer Engineering, University of Utah, 50 South Central Campus Drive, Room 3280, Salt Lake City, UT 84112

[¶]Huntsman Cancer Institute, Department of Neurosurgery, University of Utah, 2000 E. Circle of Hope Drive, Salt Lake City, UT 84112

[§]Center for Biomolecular Interaction Analysis, University of Utah, School of Medicine 4A417, 40 N. Medical Drive, Salt Lake City, UT 84132

[‖]Department of Chemistry and Biochemistry, University of Arizona, 1306 E. University Boulevard, Tucson, AZ 85721

[⊥]Salt Lake City Bioscience, 2828 SW Corbett Avenue #116, Portland, OR 97201

Abstract

Methylation of DNA is responsible for gene silencing by establishing heterochromatin structure that represses transcription, and studies have shown that cytosine methylation of CpG islands in promoter regions acts as a precursor to early cancer development. The naturally occurring methyl binding domain (MBD) proteins from mammals are known to bind to the methylated CpG dinucleotide (mCpG), and subsequently recruit other chromatin-modifying proteins to suppress transcription. Conventional methods of detection for methylated DNA involve bisulfite treatment or immunoprecipitation prior to performing an assay. We focus on proof-of-concept studies for a direct microarray-based assay using surface-bound methylated probes. The recombinant protein 1xMBD-GFP recognizes hemi-methylation and symmetric methylation of the CpG sequence of hybridized dsDNA, while displaying greater affinity for the symmetric methylation motif, as evaluated by SPR. From these studies, for symmetric mCpG, the K_D for 1xMBD-GFP ranged from 106 nM to 870 nM, depending upon the proximity of the methylation site to the sensor surface. The K_D values for non-symmetrical methylation motifs were consistently greater (> 2 μM), but the binding selectivity between symmetric and hemi-methylation motifs ranged from 4 to 30, with reduced selectivity for sites close to the surface or multiple sites in proximity, which we attribute to steric effects. Fitting skew normal probability density functions to our data, we estimate an accuracy of 97.5% for our method in identifying methylated CpG loci, which can be improved through optimization of probe design and surface density.

Introduction

In eukaryotic DNA, cytosine-guanine sequences (CpGs) are often found with the cytosine methylated at carbon 5 (m^5C). Symmetric methylation of CpG motifs in genomic DNA is a

[*]To whom correspondence should be addressed, blair@ece.utah.edu.

general mechanism of gene silencing and epigenetic inheritance. Up to 85% of CpGs in exons, transposons, and microsatellites are methylated in normal mammalian cells.[1–3] It is probable that methylation prevents the expression of parasitic sequences and of "accidental" promoter sequences in exons.[4] Methylation plays a role in inactivating the X chromosome in females;[5] it also appears to play a critical role in development.[6–8] However, methylation is a rare event in CG-rich regions of promoters or transcription initiation sequences, which are usually referred to as CpG islands. The situation is significantly different in cancer cells, where massive methylation of promoter regions is frequently observed,[9,10] silencing gene expression. The latter situation was studied in the context of transcriptional repression of tumor suppressor and DNA repair genes. Correlations between promoter methylation levels and tumorigenesis were established for various types of tumors in different tissues, which makes methylated CpG islands promising biomarkers for diagnosis and prognosis of many cancers.[11–14]

Three basic approaches are used to assess methylation levels of CpG islands: methylation-specific DNA restriction digests;[15] bisulfite treatment, followed by quantitative PCR,[16] sequencing,[17] or microarray analysis;[13,18] and enrichment of sample for methylated sequences, followed by microarray analysis19–21 or PCR.[22] Restriction digests with methylation-sensitive restriction endonucleases are biased and limited according to the palette of restriction enzymes available. These digests serve primarily as a qualitative approach (yes or no answer) based on changes in restriction cleavage sites; the other methods attempt to quantify methylation.

A number of methods rely on differences in deamination patterns of methylated and unmethylated cytocines when subjected to bisulfite treatment: unmethylated cytocines undergo deamination to produce a C to U transition, while methylated cytocines are resistant to deamination. With the development of qPCR, this approach provides quantitative data on methylation status of the targets. This method, however, has limitations - namely, it is necessary to perform two amplifications in parallel for each CpG within the sequence (gene) of interest. The CpG island of a typical promoter may contain hundreds of CpGs; thorough scanning of just one such island requires >100 separate qPCR reactions. Moreover, for meaningful quantification, the efficiencies of all qPCR reactions must be matched (corrections based on calculated efficiency differences are not reliable). These limitations may be circumvented somewhat by using melting curve analysis.23 Methylation specific sequencing17 remains the gold standard; however, if the sample originates from heterogeneous tissue (as is usually the case with solid tumor biopsies or excisions), results of sequencing are often ambiguous and rarely quantitative. Other bisulfite methods are primarily based upon bisulfite pre-treatment of the sample, followed by hybridization to an array of sequence specific oligonucleotide probes. Detection may be based either on fluorescence readout,13,18 single-nucleotide extension (SNuPE),24 or mass spectrometric methods.25 A significant limitation of all bisulfite-based approaches is the duration of bisulfite treatment, which usually takes ~16 hours and requires rigorous control for complete deamination.26

Recently, significant attention has been directed towards other microarray-based methods of methylation analysis. The capability of microarrays to monitor many genetic loci has been shown to be an efficient screening technique for a large number of targets; however, current microarray technologies lack reliable quantitation and require time-consuming preprocessing, both of which limit its usefulness in analytical and clinical applications. These methods start by dividing sheared sample DNA (sheared into appropriately-sized fragments) into two portions. One portion is kept as a reference, while the other is enriched for methylated sequences. In methylated DNA immunoprecipitation (MeDIP), methylated sequences are precipitated by a monoclonal antibody raised against m^5C.19,20,27 The precipitated DNA is extracted and labeled with one fluorescent dye while the non-enriched DNA is labeled with another. Both samples are then denatured and hybridized onto a microarray. By comparing the

relative intensities of each fluorescent color at each position of the array, the degree of methylation of many genetic loci can be determined semi-quantitatively. A similar technique, the methylated CpG-island recovery assay (MIRA), uses proteins that bind specifically to symmetrically methylated CpG motifs.[21] These methyl-binding domain (MBD) proteins are covalently bound to a solid support (such as Sepharose beads) and packed into a chromatography column. Half of the sample is then enriched by affinity chromatography, i.e. methylated sequences stick to the beads and unmethylated ones do not (methylated DNA pull-down assay). Elution yields methylation enriched DNA, which is then processed and hybridized along with non-enriched DNA as in MeDIP. Enrichment can also be performed directly in a PCR reaction vessel.22

Two families of mammalian gene products exhibit specificity in binding to CpG islands of genomic DNA. One family is represented by proteins containing a methyl-binding domain (MBD) and consists of MBD1, MBD2, MBD4 and MeCP2,28–30 while another is represented by Kaiso proteins with characteristic zinc-finger motif. 31 MBD proteins have been investigated extensively as part of the mechanism of gene silencing and with regard to their modulation of other chromatin functions (resistance to DNaseI-dependent removal of nucleosomes).32 Data on sequence preferences for MBD binding suggest that their sequence specificities are not significant.33 Methyl-binding proteins have been engineered by fusing a purification tag to monomeric or polymeric MBD1 methyl-binding domains. Constructs included one (1xMBD) to four MBDs in a single polypeptide. These engineered MBD proteins demonstrate significant specificity of CpG recognition, suggesting that MBDs may be used as sensitive analytical tools for detection of methylated CpG islands.34–37

The purpose of this paper is to present proof-of-principle results for a new method to profile DNA methylation patterns, without the need for bisulfite treatment or other enrichment steps, by using direct MBD binding to surface-bound dsDNA. This method is based upon immobilizing single-stranded capture oligos, methylated at known CpG locations, on the array. Subsequent hybridization with sample ssDNA creates hybrids at the surface with varying states of symmetric and hemi-methylation, but with no more than one symmetric methylation site per probe. The preferential binding of MBD proteins to a symmetric methylation site is used to determine the methylation state of the sample at that site. As illustrated in Figure 1, this microarray-compatible method yields not only the sequence information of the unknown sample, but also the methylation status at each CpG locus in the particular sequence. Here, we estimate the equilibrium dissociation constant, K_D, for MBD protein binding to dsDNA with different methylation motifs in order to quantify binding selectivity and sensitivity. We use a surface plasmon resonance (SPR) platform to monitor protein binding to dsDNA, where implementation on a fluorescence microarray platform[37,38] is the ultimate end goal due to its greater scalability and better detection sensitivity.

Materials and Methods

Protein Expression

Recombinant plasmids pET30(b+)-1xMBD were received from Adrian Bird's lab (Edinburgh, UK). The 1xMBD plasmid encodes the N-terminal nuclear localization signal, a 6-His tag followed by the cDNA of MBD1 amino acids 1–75, and a C-terminal HA epitope tag. For the 1xMBD-GFP construct, the GFP gene from the pUB-GFP plasmid (Addgene, #11155)[39] was amplified and inserted into the 1xMBD plasmid, downstream of the MBD gene fragment in place of the HA gene. Incorporation of the GFP gene was performed at this stage in order to study a construct that would be readily applicable to a fluorescence microarray implementation of the assay. Transformations of the recombinant plasmids were performed with *E. Coli* strain BL21DE3(pLyS) according to instructions from the manufacturer. A 450 mL LB medium was inoculated with 5 mL starter culture, and recombinant protein was induced at OD600 of 0.5–

1 with final concentration of 1 mM IPTG, and then incubated at 37°C for 3 hours. The cell cultures were subsequently centrifuged at 6000g at 4°C. The cell pellets were treated with Bugbuster solution with Benzonase nuclease per manufacturer's instruction to lyse cell membranes, followed by centrifugation at 12,000g for 20 minutes to separate the supernatant from the insoluble fractions. Supernatant containing the protein was mixed with buffer containing 300 mM NaCl, 100 mM NaH_2PO_4, 10 mM Tris, 10 mM BME, and 10 mM imidazole, then loaded onto a Ni-NTA column followed by buffer wash. Protein was removed from the Ni column with 4–6 mL of elution buffer (300 mM NaCl, 100 mM NaH_2PO_4, 10 mM Tris, 10 mM BME, and 250 mM imidazole), and dialyzed into PBS/10% glycerol buffer with 1 mM dithiothreitol. Trace impurities in the samples were separated on a Superdex gel column (Pharmacia) to obtain higher purity of MBD protein. Protein concentration was measured via Bradford assay. Cell pellets and protein samples were stored at −20°C.

The presence of MBD protein based on molecular weight was confirmed by running PAGE with 4%–12% gradient gel. To test binding of the MBD protein, an electrophoretic mobility shift assay (EMSA) was used to detect a bandshift. In each experiment, 1–4 nmoles of purified MBD protein was pre-incubated in binding buffer of 10 mM HEPES, 3 mM $MgCl_2$, 10% glycerol, 1 mM dithiothreitol, and 100 mM KCl at room temperature for 10 minutes, before adding pre-hybridized dsDNA of 0.4–1 nmole. Three different DNA-methylation motifs were used: non-methylated, hemi-methylated, and symmetrically methylated. After incubation for 2 hours at room temperature, the binding solutions were loaded on 2% agarose/0.5X TBE at 4°C and run for 2 hours at 7 V/cm electric field. Upon detection of bandshift in EMSA, protein samples were used for SPR experiments.

Preparation of Oligos

For testing the binding of MBD proteins with methylated DNA, we chose CpG-rich target oligonucleotide sequences from the O6-methylguanine DNA methyltransferase (MGMT) gene and promoter region. The methylation status of the promoter region, in particular, has predictive significance to the treatment of glioblastoma multiforme (GBM), which is the most common and malignant brain tumor (survival rate of less than 5% at five years after presentation40). Radiation and some forms of alkylating chemotherapy are employed in the treatment of GMB. Patients receiving radiotherapy alone have lower survival rate compared to patients who received radiotherapy plus temozolomide (TMZ);41 TMZ and BCNU (1,3-bis (2-chloroethyl)-1-mitrosurea) are methylating/alkylating agents widely used for treatment of GBM.42 Long-term survivors (those living for 3 to 5 years) are characterized with hypermethylation of the MGMT promoter;43 MGMT is a DNA repair enzyme that confers cancer cell resistance to guanine O6-alkylating agent-based chemotherapy. MGMT expression levels are a major predictor of TMZ sensitivity in human glioma cell lines and tumors taken from human patients.44,45 There is evidence that methylation of the promoter of the MGMT-gene in even low-grade astrocytomas and oligodendrogliomas predicts response to TMZ.46

DNA probes and complementary targets with particular methylation patterns were synthesized at the DNA/Peptide Synthesis Facility at the University of Utah (Table 1 and Table 2). In the tables, the methylation patterns are indicated with an 'm' for a methylated CpG locus and an 'o' for a non-methylated locus. The oligos were reconstituted in PBS buffer with 1 mM EDTA for long-term storage, and target oligos for hybridization were diluted to 1 μM in 3xSSC. In order to examine potential steric hindrance effects, a longer m_o_o probe (25-mer) was used for comparison with the 22-mer m_o_o. The methylation site of the longer m_o_o* probe was situated 8 bases away from the 5' end of the strand, with only a 4 base distance for the 22-mer m_o_o. The 39-mer target sequence arises from cutting the MGMT promoter region with the restriction enzymes EcoNI and AluI. The sequence in Table 2 has methylation sites situated closer to each other than the sequence from Table 1.

SPR Experiments

SPR was used to measure binding kinetics for 1xMBD-GFP, and all SPR experiments were carried out on a ProteOn XPR36. Matrix experiments were carried out with the probe and target sequences from Table 1 and Table 2. In the first SPR experiment (Matrix I), a monolayer of streptavidin was built on the GLC chip using streptavidin concentration of ~95 nM. Then six biotinylated probes at 125 nM were captured on the channel surfaces at a flow rate of 30 μL/min for 6 minutes. The flow cell was then rotated 90°, followed by hybridization of six target DNA sequences at 25 μL/min for 6 minutes, or until the RU reached equilibrium. A total of 36 target/probe dsDNA combinations were generated. After hybridization of the target ssDNA, the average RU was 590, with standard deviation of 200. In the second SPR experiment (Matrix II), binding of 1xMBD-GFP was tested with the promoter sequence along with one positive control (o_o_m/m_m_m). In these experiments, the average RU after hybridization was 1030, with standard deviation 130.

For protein binding, 1xMBD-GFP binding was performed with a flow rate of 50 μL/min for a contact time of 48 seconds, and dissociation of 6 minutes by the running buffer (10 mM HEPES, 3 mM $MgCl_2$, 10% glycerol, 1 mM dithiothreitol, 100 mM KCl, 0.1% BSA, and 0.01% Tween-20) until the RU stabilized. The protein binding started from the lowest concentration (2.7 nM) to the highest (2 μM) in a 3-fold dilution series, and the binding-series was performed twice on the same chip. Using Scrubber 2.0, kinetic model fitting (Langmuir 1:1) was performed based on the RU curves from the two experiments, allowing binding site concentration (i.e. surface-bound dsDNA) to be a free-parameter for each of the 36 combinations.

Results and Discussion

Sensorgrams of 1xMBD-GFP binding are presented in Figure 2 and Figure 3, along with the corresponding average K_D values and standard deviations summarized in Table 3 and Table 4, respectively.

Based on the extracted K_D values, clear differentiation between symmetric and non-symmetric methylation motifs is obtained, as quantified below; however the distance between the methylation site and the chip surface affects the sensitivity and selectivity of 1xMBD-GFP binding. For the m_o_o/m_o_o and m_o_o*/m_o_o probe/target motifs, the methylated cytosine was positioned 4-bp and 8-bp away from the surface, respectively. From Table 3, the K_D value was considerably lower for the symmetrical methylation site in m_o_o*, corresponding to 4.8-fold higher sensitivity than the m_o_o counterpart. We attribute this phenomenon to steric hindrance, where the protein has limited access to the end of the dsDNA strand that is adjacent to the surface. The steric hindrance effect appeared to increase as the distance of the methyl group from the surface decreased. For the m_o_o* , o_m_o, and o_o_m symmetrical methylation motifs (including nearby hemi-methyl groups), the average K_D values were about 656 nM, 298 nM, and 161 nM, respectively. In the case of the promoter sequence experiment, for the m_o_o_o, o_m_o_o, o_o_m_o and o_o_o_m symmetrical methylation motifs, the average K_D was about 561 nM, 346 nM, 140 nM, and 281 nM, respectively.

Furthermore, it appears that the MBD protein does not efficiently recognize double symmetrical methylation sites that are positioned in close proximity on a dsDNA strand, as suggested by the probe/target motifs o_m_m/m_o_m and o_m_m/o_m_m, for which the K_D values were closely matched (0.15 and 0.16 μM). This is indicative of a proximity effect, when two methylation sites are too close to each other with respect to the size of the 1xMBD molecule, protein binding to one of the methyl groups blocks access to the other one. Nevertheless, the K_D values from other probe motifs yield relevant information regarding the presence of another methyl group on the target ssDNA, which is the basis of our profiling

method (i.e. singly-methylated probes are sufficient). Comparison of the K_D values for o_o_m/o_m_m and o_m_o/o_m_m confirms the double symmetric methylation motif of the target.

In terms of the K_D analysis, it should be noted that the K_D values are clustered into two groups - one group for symmetric methylation motifs (K_D < 1 μM) and the other group for non-symmetric methylation motifs (K_D >2 μM). In order to estimate the accuracy of the profiling method in identifying target methylation state, we fit these two groups of K_D values to skew-normal probability density functions. Figure 4 shows the histograms of the two populations along with the corresponding pdfs. Choosing a threshold K_D value of 0.9 μM, we can evaluate the false positive and false negative rates as 1.5% and 1.0%, respectively, with an overall call accuracy of 97.5%.

The K_D value of 1xMBD-GFP binding to symmetric methylation CpG sites from our SPR study, with an average value of 0.33 μM, is consistent with solution measurements of the MBD family.[47] Further, we obtained average K_D ratio between non-methylation and symmetric methylation of greater than 150:1, and average ratio of 18:1 between hemi-methylation and symmetric.

Conclusions

Traditional DNA methylation assays have been dependent on either bisulfite treatment or enrichment of the methylated DNA strand by MeDIP. While these are standard methods in detection and/or quantification of DNA methylation, bisulfite conversion has shown sequence bias leading to incomplete conversion of non-methylated cytosines. In addition, both bisulfite and differential PCR experiments are time consuming and labor intensive; hence, there is an open opportunity for a sensitive method that can detect DNA methylation that bypasses the bisulfite treatment or enrichment steps.

MBD proteins have been known to recognize mCpG sites on the promoter region. By applying this natural property of the MBD protein, we have developed a direct detection method for methylated dsDNA. Our experimental validation with SPR has shown that the 1xMBD-GFP protein recognizes both hemi and symmetric methylation on a surface-bound hybridized dsDNA strand. Furthermore, MBD binding consistently exhibits selectivity for the symmetrical methylation motif. However, the sensitivity and selectivity are both influenced by steric hindrance. This effect can be mitigated somewhat through probe design, for which the methylated loci of the probe can be placed far enough from the surface to allow for access by the protein molecule. This suggests that there may be a number of optimized conditions for the ssDNA capture probe based upon the density of immobilization. In the case of a fluorescence microarray surface, the density of a reactive silane (e.g. APTES or GPS) can be varied by dilution with another monofunctional “spacer” silane;[48] this in turn affects the density of the probe through its covalent linkage to the reactive silane.

While SPR has sufficient sensitivity to protein binding, throughput is limited in the number of individual reactions and sensitivity to DNA hybridization is typically less than obtained with fluorescence microarray experiments. As for diagnostic applications, a fluorescence microarray slide can accommodate a high density layout, and can serve as a fast and efficient screening tool for methylated CpG loci in DNA from tissue samples. The ideal microarray platform would perform real-time fluorescence readout, analogous to SPR, with which on and off rates from binding of MBD at multiple concentrations could accurately recover K_D at each CpG locus. In this scenario, we estimate 97.5% accuracy (or better, with assay optimizations) in calling the methylation state at any given locus. Further, by labeling the target ssDNA and MBD with spectrally distinct fluorophores, the calibrated fluorescence ratio (compared to positive and negative controls) could be used to identify methylation state. This approach would

be suitable for the more conventional endpoint microarray experiments, using a single MBD concentration less than approximately 0.33 μM to maximize discrimination.

Acknowledgments

The authors thank Prof. A. Bird for providing 1xMBD plasmid. This research was supported in part by grants 4R44GM084603-02 and R21CA143661 from the NIH.

References

1. Bird A. Cell 1992;70:5–8. [PubMed: 1377983]
2. Cedar H. Cell 1988;53:3–4. [PubMed: 3280142]
3. Lewin B. Cell 1998;93:301–303. [PubMed: 9590160]
4. Bird A. Genes & Development 2002;16:6–21. [PubMed: 11782440]
5. Grant SG, Chapman VM. Annual Review of Genetics 1988;22:199–233.
6. Li E, Bestor TH, Jaenisch R. Cell 1992;69:915–926. [PubMed: 1606615]
7. Okano M, Bell DW, Haber DA, Li E. Cell 1999;99:247–257. [PubMed: 10555141]
8. Stancheva, v; Meehan, RR. Genes & Development 2000;14:313–327. [PubMed: 10673503]
9. Esteller M, Corn PG, Baylin SB, Herman JG. Cancer Research 2001;61:3225–3229. [PubMed: 11309270]
10. Esteller M, Fraga MF, Paz MF, Campo E, Colomer D, Novo FJ, Calasanz MJ, Galm O, Guos M, Benitez J, Herman JG, Croce LD, Pelicci PG. Science 2002;297:1807d–1808d. [PubMed: 12229925]
11. Costello JF, et al. Nature Genetics 2000;24:132–138. [PubMed: 10655057]
12. Ordway J, et al. Carcinogenesis 2006;27:2409–2423. [PubMed: 16952911]
13. Gebhard C, Schwarzfischer L, Pham T-H, Schilling E, Klug M, Andreesen R, Rehli M. Cancer Research 2006;66:6118–6128. [PubMed: 16778185]
14. Shames DS, Minna JD, Gazdar AF. Cancer Letters 2007;251:187–198. [PubMed: 17166656]
15. McClelland M, Nelson M. Nucleic Acids Research 1985;13:r201–r207. [PubMed: 2987886]
16. Herman JG, Graff JR, Myöhänen S, Nelkin BD, Baylin SB. Proceedings of the National Academy of Sciences 1996;93:9821–9826.
17. Frommer M, McDonald LE, Millar DS, Collis CM, Watt F, Grigg GW, Molloy PL, Paul CL. Proceedings of the National Academy of Sciences 1992;89:1827–1831.
18. Gitan RS, Shi H, Chen C-M, Yan PS, Huang TH-M. Genome Research 2002;12:158–164. [PubMed: 11779841]
19. Keshet I, Schlesinger Y, Farkash S, Rand E, Hecht M, Segal E, Pikarski E, Young RA, Niveleau A, Cedar H, Simon I. Nature Genetics 2006;38:149–153. [PubMed: 16444255]
20. Weber M, Davies JJ, Wittig D, Oakeley EJ, Hase M, Lam WL, Schübeler D. Nature Genetics 2005;37:853–862. [PubMed: 16007088]
21. Rauch T, Li H, Wu X, Pfeifer GP. Cancer Research 2006;66:7939–7947. [PubMed: 16912168]
22. Gebhard C, Schwarzfischer L, Pham TH, Andreesen R, Mackensen A, Rehli M. Nucleic Acids Research 2006;34:e82. [PubMed: 16822855]
23. Lorente A, Mueller W, Urdangarin E, Lázcoz P, von Deimling A, Castresana J. BMC Cancer 2008;8:61. [PubMed: 18298842]
24. Gonzalgo M, Jones P. Nucleic Acids Research 1997;25:2529–2531. [PubMed: 9171109]
25. Schatz P, Distler J, Berlin K, Schuster M. Nucl. Acids Res 2006;34:e59. [PubMed: 16670426]
26. Kristensen LS, Hansen LL. Clinical Chemistry 2009;55:1471–1483. [PubMed: 19520761]
27. Oakeley EJ, Podestà A, Jost J-P. Proceedings of the National Academy of Sciences of the United States of America 1997;94:11721–11725. [PubMed: 9326677]
28. Meehan RR, Lewis JD, McKay S, Kleiner EL, Bird AP. Cell 1989;58:499–507. [PubMed: 2758464]
29. Lewis JD, Meehan RR, Henzel WJ, Maurer-Fogy I, Jeppesen P, Klein F, Bird A. Cell 1992;69:905–914. [PubMed: 1606614]
30. Hendrich B, Bird A. Genetical Research 1998;72:59–72. [PubMed: 9867472]

31. Klose RJ, Bird AP. Trends in Biochemical Sciences 2005;31:89–97. [PubMed: 16403636]
32. Nan X, Ng H-H, Johnson CA, Laherty CD, Turner BM, Eisenman RN, Bird A. Nature 1998;393:386–389. [PubMed: 9620804]
33. Jorgensen HF, Ben-Porath I, Bird AP. Molecular and Cellular Biology 2004;24:3387–3395. [PubMed: 15060159]
34. Jorgensen HF, Adie K, Chaubert P, Bird AP. Nucleic Acids Research 2006;34:e96. [PubMed: 16893950]
35. Stains CI, Furman JL, Segal DJ, Ghosh I. Journal of the Americal Chemical Society 2006;128:9761–9765.
36. Porter JR, Stains CI, Segal DJ, Ghosh I. Analytical Chemistry 2007;79:6702–6708. [PubMed: 17685552]
37. Luo J, Zheng W, Wang Y, Wu Z, Bai Y, Lu Z. Analytical Biochemistry 2009;387:143–149. [PubMed: 19084498]
38. Bishop J, Chagovetz AM, Blair S. Biophysical Journal 2008;94:1726–1734. [PubMed: 17993490]
39. Matsuda T, Cepko CL. Proceedings of the National Academy of Sciences of the United States of America 2004;101:16–22. [PubMed: 14603031]
40. Surawicz TS, Davis F, Freels S, Laws ER, Menck HR. Journal of Neuro-Oncology 1998;40:151–160. [PubMed: 9892097]
41. Stupp R, et al. New England Journal of Medicine 2005;352:987–996. [PubMed: 15758009]
42. Bandres E, Andion E, Escalada A, Honorato B, Catalan V, Cubedo E, Cordeu L, Garcia F, Zarate R, Zabalegui N, Garcia-Foncillas J. Journal of Neuro-Oncology 2005;73:189–198. [PubMed: 15980968]
43. van den Bent MJ, Hegi ME, Stupp R. European Journal of Cancer 2006;42:582–588. [PubMed: 16427778]
44. Hegi ME, et al. The New England Journal of Medicine 2005;352:997–1003. [PubMed: 15758010]
45. Hermisson M, Klumpp A, Wick W, Wischhusen J, Nagel G, Roos W, Kaina B, Weller M. Journal of Neurochemistry 2006;96:766–776. [PubMed: 16405512]
46. Levin N, Lavon I, Zelikovitsh B, Fuchs D, Bokstein F, Fellig Y, Siegal T. Cancer 2006;106:1759–1765. [PubMed: 16541434]
47. Fraga MF, Ballestar E, Montoya G, Taysavang P, Wade PA, Esteller M. Nucleic Acids Research 2003;31:1765–1774. [PubMed: 12626718]
48. Wayment JR, Harris JM. Analytical Chemistry 2006;78:7841–7849. [PubMed: 17105178]

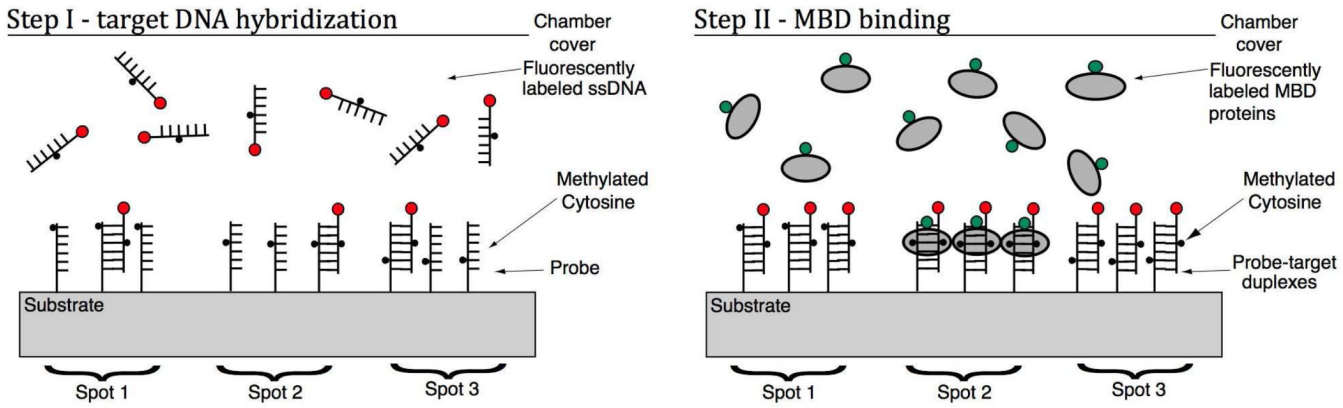

Figure 1.

Illustration of the two-step methylation profiling assay. Capture probe oligonucleotides are singly-methylated at all CpG loci. The first step is similar to a conventional DNA assay in that sample ssDNA, of unknown methylation status, is hybridized to the capture array. Hybridization may be quantified by fluorescence detection or SPR, for example. In the second step, binding of MBD protein is performed, with quantification via fluorescence (under excitation from a second laser) or SPR.MBD preferentially binds to symmetric methylation sites (i.e. where the methylation states of the target and probe overlap). By comparing the (calibrated) sensor response from the MBD protein to that of the dsDNA at each capture spot, the methylation status can be determined at each CpG location.

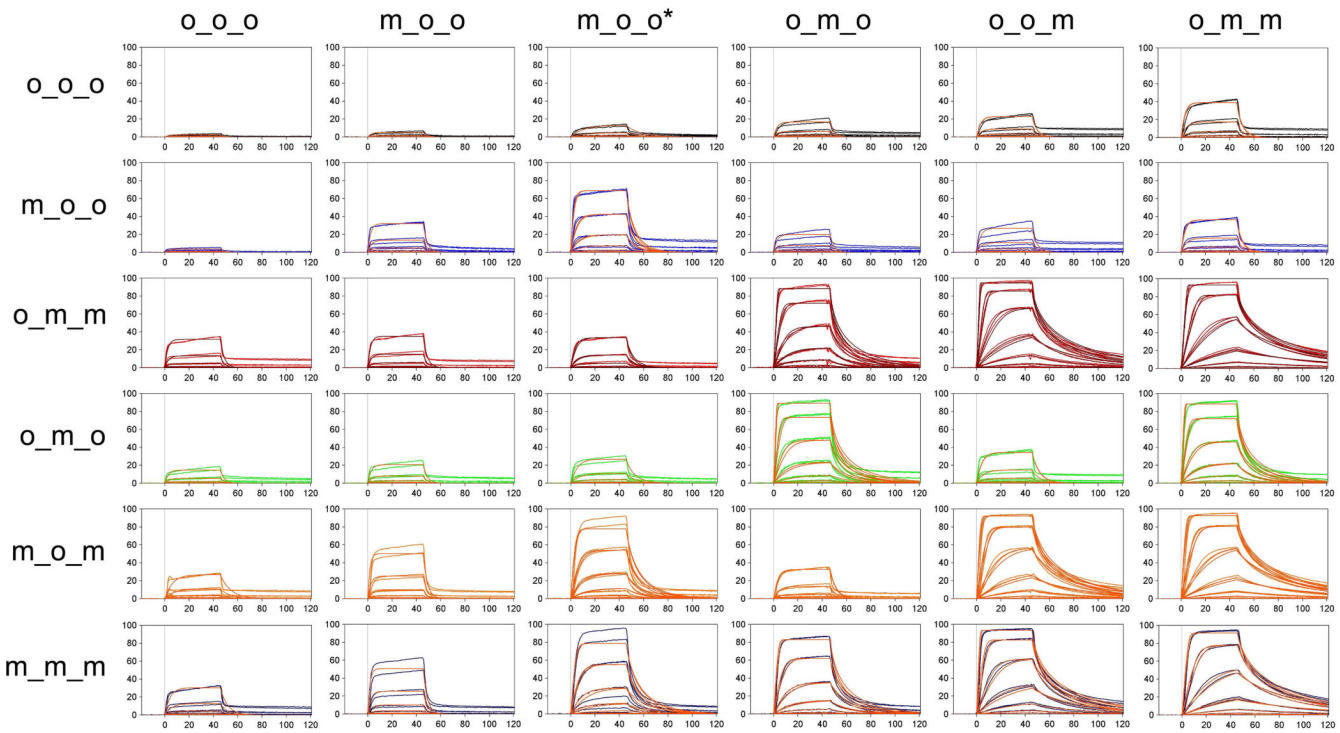

Figure 2.

SPR sensorgrams for 1xMBD-GFP binding to the dsDNA matrix for the MGMT gene sequence, with normalized RU (y-axis) versus time (x-axis). Each column represents a different probe methylation pattern, and each row, a different target methylation pattern.

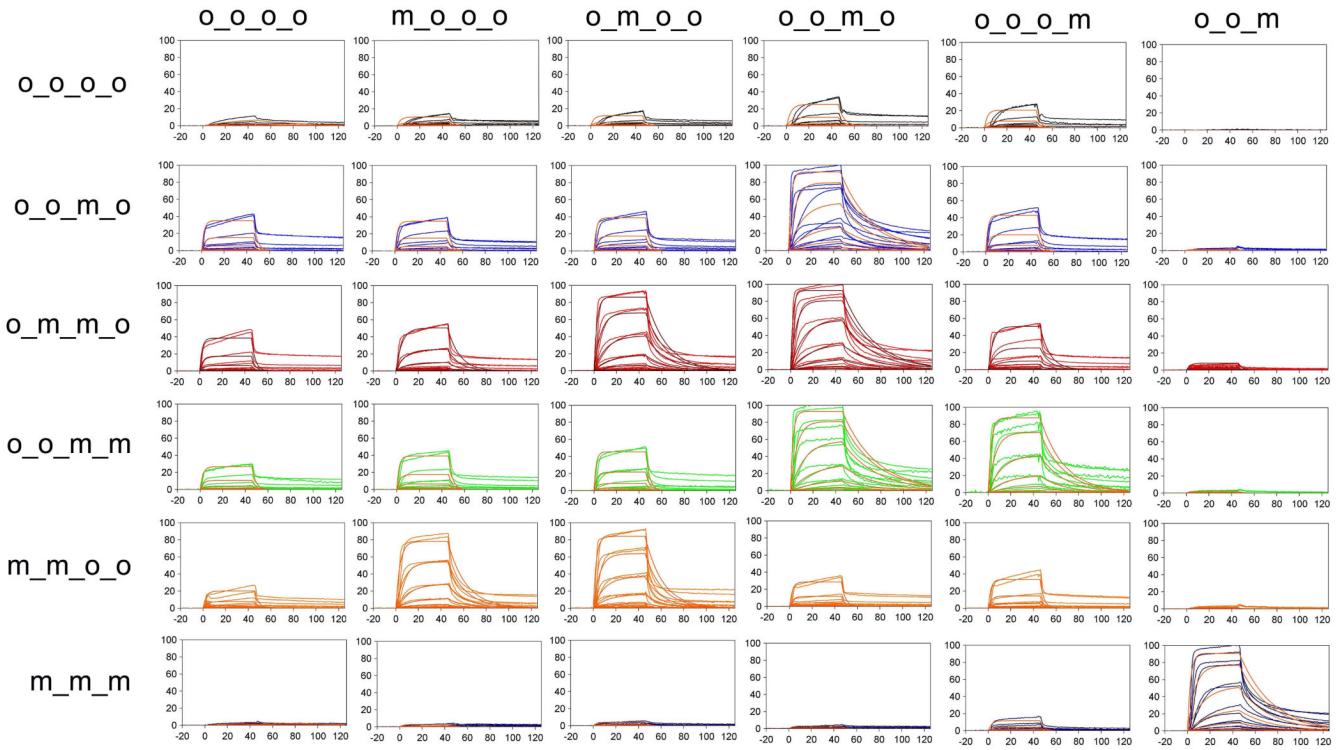

Figure 3.

SPR sensorgrams for 1xMBD-GFP binding to the dsDNA matrix for the MGMT promoter sequence, with normalized RU (y-axis) versus time (x-axis). Each column represents a different probe methylation pattern, and each row, a different target methylation pattern.

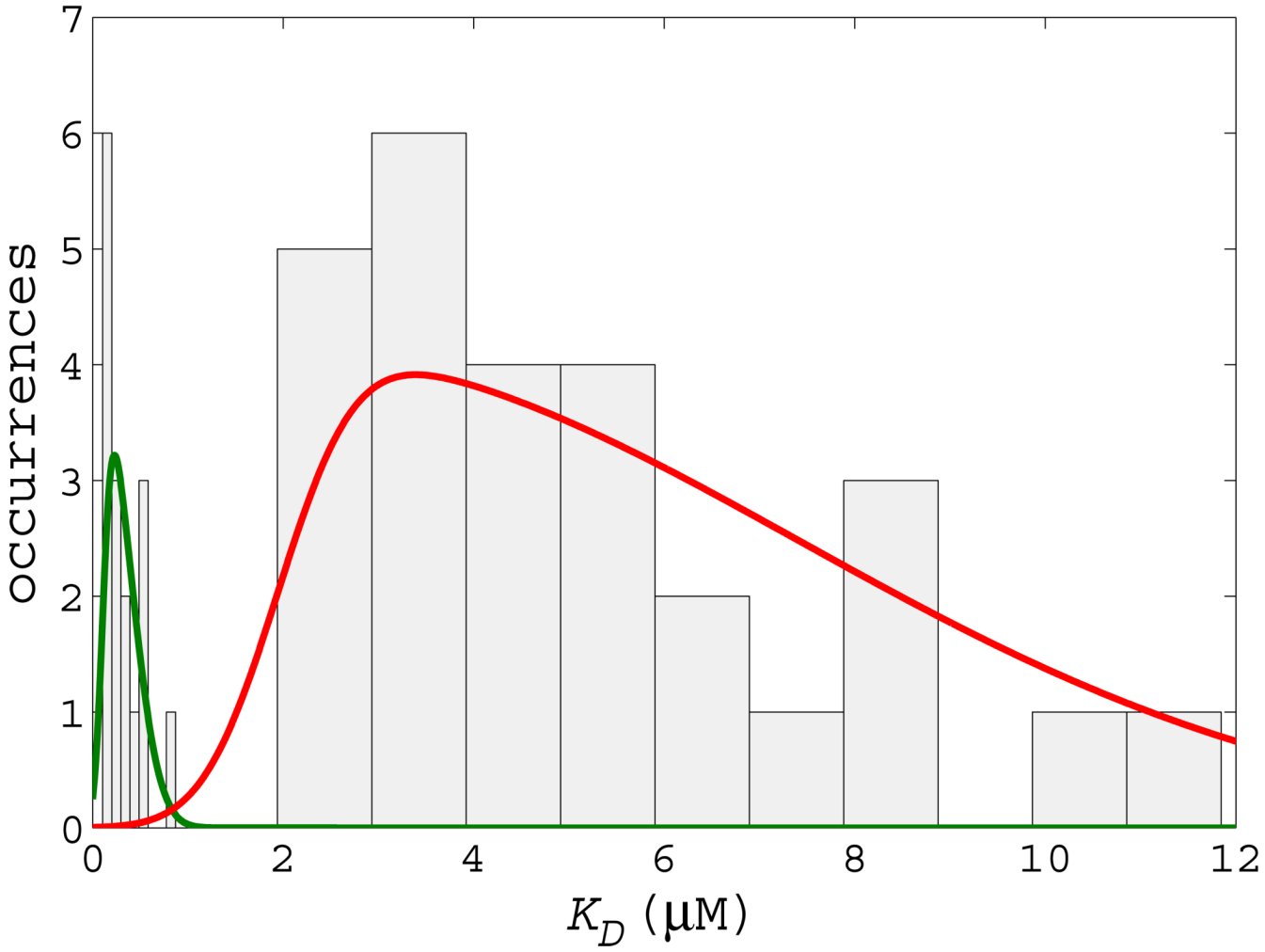

Figure 4.

Histogram of the K_D population obtained from SPR experiments for both the gene and promoter sequences. Each group, symmetric methylation and non-symmetric methylation, was fitted to a skew-normal probability density function. These pdfs were scaled before plotting in order to match the histogram scale; prior to any error calculations, the pdfs were normalized to integrate to 1.

Table 1

Test sequence derived from the MGMT gene. Subscript *m* represents a methylated cytosine base. For probes used with SPR, the 5’ end is modified with biotin.

Oligo Type	Pattern	Sequence
Probe	o_o_o	5’-TTTGCGGTCCGCTGCCCGACCC-3’
Probe	o_o_m	5’-TTTGCGGTCCGCTGCC$_m$CGACCC-3’
Probe	o_m_o	5’-TTTGCGGTC$_m$CGCTGCCCGACCC-3’
Probe	m_o_o	5’-TTTG$_m$CGGTCCGCTGCCCGACCC-3’
Probe	m_o_o*	5’-GTAGTTTG$_m$CGGTCCGCTGCCCGACC-3’
Probe	o_m_m	5’-TTTGCGGTC$_m$CGCTGCC$_m$CGACCC-3’
Target	o_o_o	3’-AAACGCCAGGCGACGGGCTGGG-Cy5
Target	m_o_o	3’-AAACGC$_m$CAGGCGACGGGCTGGG-Cy5
Target	o_m_m	3’-AAACGCCAGGC$_m$GACGGGC$_m$TGGG-Cy5
Target	o_m_o	3’-AAACGCCAGGC$_m$GACGGGCTGGG-Cy5
Target	m_o_m	3’-AAACGC$_m$CAGGCGACGGGC$_m$TGGG-Cy5
Target	m_m_m	3’-AAACGC$_m$CAGGC$_m$GACGGGC$_m$TGGG-Cy5

Table 2

Test sequence derived from the MGMT promoter region. Subscript *m* represents a methylated cytosine base. For probes used with SPR, the 5’ end is modified with biotin

Oligo Type	Pattern	Sequence
Probe	o_o_o_o	5’-GAAGTCAACAGGACGGACGCCGCGCAA-3’
Probe	o_o_o_m	5’-GAAGTCAACAGGACGGACGCCG$_m$CGCAA-3’
Probe	o_o_m_o	5’-GAAGTCAACAGGACGGACGC$_m$CGCGCAA-3’
Probe	o_m_o_o	5’-GAAGTCAACAGGACGGA$_m$CGCCGCGCAA-3’
Probe	m_o_o_o	5’-GAAGTCAACAGGA$_m$CGGACGCCGCGCAA-3’
Target	o_o_o_o	3’-TCTCCTTCAGTTGTCCTGCCTGCGGCGCGTTTCTTTCTC-5’
Target	o_o_m_o	3’-TCTCCTTCAGTTGTCCTGCCTGCGGC$_m$GCGTTTCTTTCTC-5’
Target	o_o_m_m	3’-TCTCCTTCAGTTGTCCTGCCTGCGGC$_m$GC$_m$GTTTCTTTCTC-5’
Target	o_m_m_o	3’-TCTCCTTCAGTTGTCCTGCCTGC$_m$GGC$_m$GCGTTTCTTTCTC-5’
Target	m_m_o_o	3’-TCTCCTTCAGTTGTCCTGC$_m$CTGC$_m$GGCGCGTTTCTTTCTC-5’

Table 3

K_D values (μM) of 1xMBD-GFP binding to the dsDNA matrix for the MGMT gene sequence. The column corresponds to six biotinylated probes with different methylation motifs, where m_o_o* is similar to m_o_o, except for the distance of the methyl group from the 5' end of the strand. Rows correspond to the six targets, which hybridize with the probes inside the ProteOn flow cell.

probe →	o_o_o	m_o_o	m_o_o*	o_m_o	o_o_m	o_m_m
o_o_o	72±5	35±1	13.1±0.3	10.0±0.1	6.8±0.1	3.09±0.02
m_o_o	48±2	4.20±0.04	0.87±0.01	8.0±0.1	5.97±0.08	3.47±0.05
o_m_m	4.28±0.05	3.67±0.03	3.74±0.06	0.252±0.002	0.116±0.001	0.139±0.007
o_m_o	12±1	5.5±0.9	5.41±0.05	0.244±0.002	2.30±0.06	0.271±0.005
m_o_m	5.7±0.3	2.08±0.02	0.564±0.004	8.6±0.1	0.179±0.001	0.169±0.002
m_m_m	4.6±0.2	2.20±0.02	0.534±0.004	0.398±0.002	0.189±0.001	0.181±0.001

Table 4

K_D values (μM) of 1xMBD-GFP binding to the dsDNA matrix for the MGMT promoter sequence. The column corresponds to six biotinylated probes with different methylation motifs. The row corresponds to the six targets, which hybridize with the probes inside the ProteOn flow cell.

probe →	**o_o_o_o**	**m_o_o_o**	**o_m_o_o**	**o_o_m_o**	**o_o_o_m**	**o_o_m**
o_o_o_o	37±2	16.8±0.5	14.7±0.4	5.86±0.09	7.6±0.2	N/A
o_o_m_o	3.66±0.05	3.51±0.03	3.12±0.04	0.106±0.001	2.65±0.03	N/A
o_m_m_o	3.19±0.03	2.4±0.09	0.315±0.004	0.158±0.003	1.94±0.02	N/A
o_o_m_m	4.5±0.1	3.11±0.03	2.40±0.04	0.156±0.002	0.281±0.007	N/A
m_m_o_o	7.5±0.2	0.561±0.006	0.377±0.007	4.97±0.07	3.94±0.06	N/A
m_m_m	N/A	N/A	N/A	N/A	N/A	0.209±0.002